TYRE EJECTA: RADIAL SIZE-FREQUENCY DISTRIBUTION, FRAGMENT SIZES AND EJECTION VELOCITIES. Kelsi N. Singer and Luke Nowicki, Department of Earth and Planetary Sciences and McDonnell Center for the Space Sciences, Washington University, St. Louis, MO 63130 (ksinger@levee.wustl.edu, mckinnon@wustl.edu).

Introduction: Europa provides a unique case study for investigating secondary cratering processes. Its relatively pristine surface makes it is easier to study secondaries from a given large primary. This helps constrain characteristics of secondary populations in general (the numbers, sizes and ranges), which can be compared to secondary crater distributions on other solar system bodies. Similar to other studies on secondary crater fields, the secondaries mapped here have a steep size-frequency distribution.

At ~44 km in diameter, with graben extending out to ~175 km, Tyre is the largest basin on Europa. This work measured the size-frequency of secondary craters as a function of radial distance from the center of Tyre. We also estimate the size and velocity of ejected fragments that formed these secondaries.

Methods: The mosaic composed of the nine Galileo frames of the Tyre region with a resolution of ~170 m/px was used for crater counting (Fig. 1). A lower limit of five pixels was used for identification of craters, which equates to the smallest mapped craters having diameters of ~850 m. Secondary crater diameters were measured geodesically in ArcGIS. There are several instances of clustered secondaries and secondaries arranged linearly. Where it was possible to distinguish individual craters they were mapped as such. 1,012 craters were above the five pixel limit and used in this study.

This work follows a similar method to those of Vickery for large craters on Mercury, the Moon and Mars [1-2] and Alpert and Melosh for Pwyll on Europa [3]. It is impossible to ascertain the original location of ejected fragments, so the center of Tyre was used for all distance calculations. This leads to an overestimate of the range and thus an overestimate of the ejection velocities.

The distances are calculated using a flat plane approximation due the short distances involved. For a ballistic trajectory, the relationship is:

$$R = (v_{ej}^2 / g)\sin(2\theta) \qquad (1)$$

where R is the distance from the primary, θ is the ejection angle (assumed to be 45°), g is surface gravity (1.31 m/s^2), and v_{ej} is the ejection velocity [4].

The size of ejected fragments was estimated from Schmidt-Holsapple crater scaling relationships [5,6]. Two scenarios, both for the gravity-dominated regime, were considered. One where the surface is non-porous is described by:

$$d = 0.76 D_{obs}^{1.2} (\sin\theta)^{-0.4} (g/U^2)^{0.2} \qquad (2)$$

where d is the fragment diameter (assuming a spherical ejecta fragment), D_{obs} is the measured secondary crater diameter, and U is impact velocity (the same as ejection velocity, v_{ej}). Although we consider the non-porous case to be the more appropriate for Europa given the surface is relatively young, we also consider a second scenario where the surface is porous, described by:

$$d = 0.753 D_{obs}^{1.28} (\sin\theta)^{-1/3} (g/U^2)^{0.277}. \qquad (3)$$

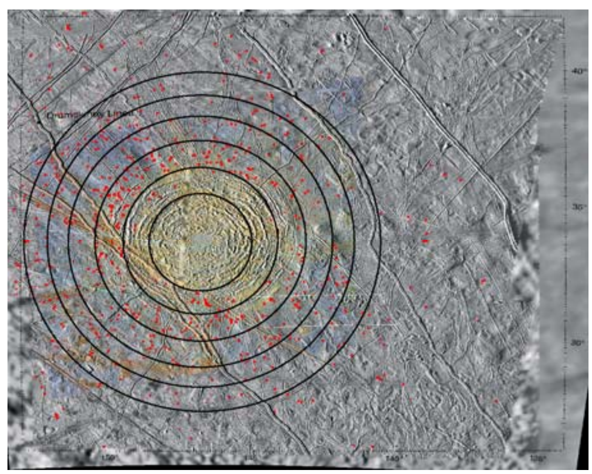

Figure 1. Map of Crater Locations. The resolution of the basemap is 170 m/px. Black rings mark 20 km distance intervals, starting at 40 km in radius and extending to 140 km in radius. The white outline marks the location of higher resolution observations which will be mapped in the future (~27 m/px).

Results: The size frequency of craters based on their radial distance from Tyre's center is presented in Fig. 2. The largest fragments are comparable to those from the similarly sized Aristillus crater on the Moon. Cumulative slopes for the craters are located in 20 km radial range bins (shown in Fig. 1) are given in Fig. 2. They range from approximate -4 to -6, with the total population having a slope of -5.

The most distant secondaries, at ~290 km, are limited by the image extent. This gives the highest ejection velocity of ~650 m/s. Ejection velocity is plotted against fragment diameter in Fig. 3. Curves of the form $d_{max} = \alpha\, v_{ej}^{-\beta}$ were fit to the maximum fragment sizes across the velocity range. For the non-porous case $d_{max} = 6.9\mathrm{x}10^5\, v_{ej}^{-1.17}$ and for the porous scenario $d_{max} = 3.0\mathrm{x}10^5\, v_{ej}^{-0.99}$. The values for the coefficient α are the same order of magnitude as found for Pwyll [3] and are several orders of magnitude smaller than α's for Mercury, the Moon and Mars (which range from 10^7-10^9) [1-2]. The values for β are comparable to the exponents found for Pwyll (-1.21 for non-porous and -1.02 for porous).

Future Work: Future work will include mapping of the higher resolution inset (shown in Fig. 1) and comparison of all data to other counts on other icy satellites. An attempt will be made to more accurately estimate ejection velocities given the fact that they did not all originate at the center of Tyre.

A compilation of secondary crater data will illuminate their overall distribution and, by extension of the relationship between d_{max} and v_{ej} to escape velocities, lead to an estimation of sesquinary sizes.

References: [1] Vickery A. M. (1986) Icarus, 67, 224-236. [2] Vickery A. M. (1987) GRL, 14, 726-729. [3] Alpert A.J. and Melosh H.J. (1999) LPSC XXX, Abstract #1881. [4] Melosh H.J. (1989) Impact Cratering: A geologic process. Oxford University Press, 87. [5] Schmidt R. M. and Holsapple K. A. (1982) GSA Spec. Pap., 190, 93-102. [6] Holsapple K. A. and Schmidt R. M. (1982) JGR, 87, 1849-1870.

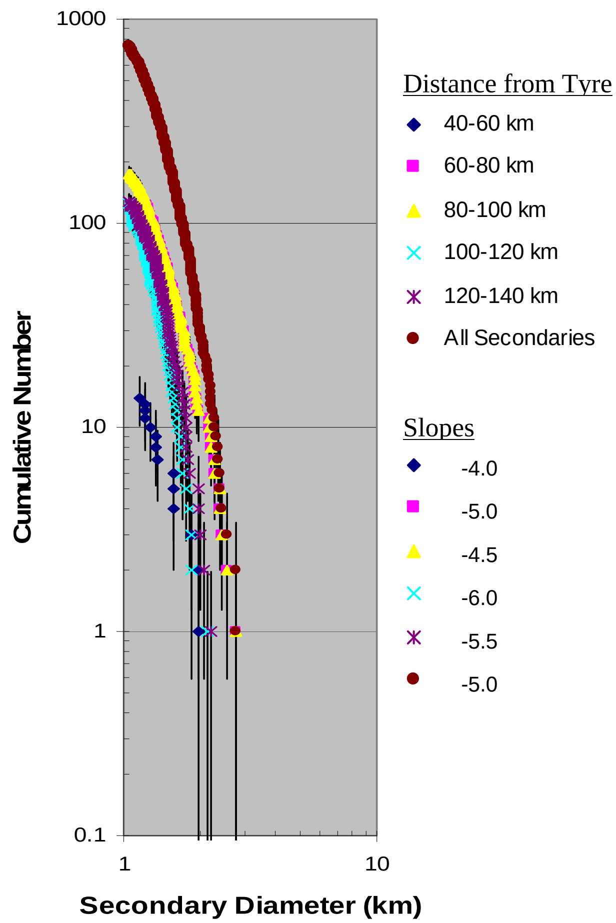

Figure 2. Size-frequency distributions for secondary craters in 20 km radial range bins.

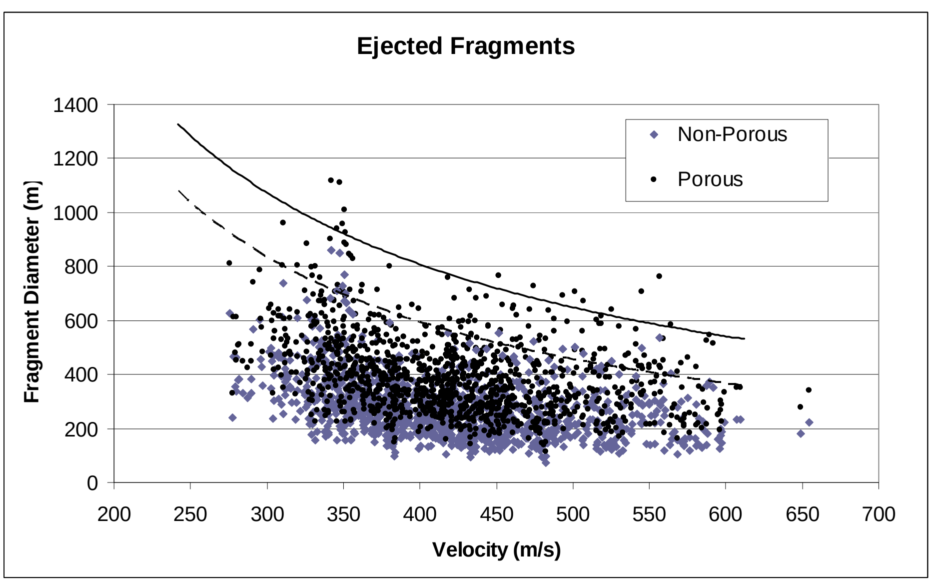

Figure 3. The velocities calculated from the distance from the center of Tyre are compared with fragment diameters calculated from the size of the secondaries. Curves of the form $d_{max} = \alpha\, v_{ej}^{-\beta}$ were fit to the maximum fragments sizes: the dashed line represents non-porous and the solid is for porous.